



HAL
open science

Cellular responses of Pacific oyster (*Crassostrea gigas*) gametes exposed in vitro to polystyrene nanoparticles

Carmen González-Fernández, Kevin Tallec, Nelly Le Goïc, Christophe Lambert, Philippe Soudant, Arnaud Huvet, Marc Suquet, Mathieu Berchel,
Ika Paul-Pont

► To cite this version:

Carmen González-Fernández, Kevin Tallec, Nelly Le Goïc, Christophe Lambert, Philippe Soudant, et al.. Cellular responses of Pacific oyster (*Crassostrea gigas*) gametes exposed in vitro to polystyrene nanoparticles. *Chemosphere*, 2018, 208, pp.764 - 772. 10.1016/j.chemosphere.2018.06.039 . hal-01813169

HAL Id: hal-01813169

<https://hal.univ-brest.fr/hal-01813169>

Submitted on 25 May 2020

HAL is a multi-disciplinary open access archive for the deposit and dissemination of scientific research documents, whether they are published or not. The documents may come from teaching and research institutions in France or abroad, or from public or private research centers.

L'archive ouverte pluridisciplinaire **HAL**, est destinée au dépôt et à la diffusion de documents scientifiques de niveau recherche, publiés ou non, émanant des établissements d'enseignement et de recherche français ou étrangers, des laboratoires publics ou privés.

Cellular responses of Pacific oyster (*Crassostrea gigas*) gametes exposed *in vitro* to polystyrene nanoparticles

González-Fernández Carmen ^{1,*}, Tallec Kevin ², Le Goïc Nelly ¹, Lambert Christophe ¹, Soudant Philippe ¹, Huvet Arnaud ², Suquet Marc ², Berchel Mathieu ³, Paul-Pont Ika ¹

¹ Laboratoire des Sciences de l'Environnement Marin (LEMAR), UMR 6539 CNRS/UBO/IRD/IFREMER, Institut Universitaire Européen de la Mer (IUEM), Rue Dumont d'Urville, 29280 Plouzané, France

² Ifremer, Laboratoire des Sciences de l'Environnement Marin (LEMAR), CS 10070, 29280 Plouzané, France

³ CEMCA, UMR CNRS 6521, IBSAM, UFR Sciences, Université de Bretagne Occidentale, 6 avenue Victor Le Gorgeu, 29238 Brest, France

* Corresponding author : Carmen González-Fernández, email address :

carmen.gonzalezfernandez@univ-brest.fr

Abstract :

While the detection and quantification of nano-sized plastic in the environment remains a challenge, the growing number of polymer applications mean that we can expect an increase in the release of nanoplastics into the environment by indirect outputs. Today, very little is known about the impact of nano-sized plastics on marine organisms. Thus, the objective of this study was to investigate the toxicity of polystyrene nanoplastics (NPs) on oyster (*Crassostrea gigas*) gametes. Spermatozoa and oocytes were exposed to four NPs concentrations ranging from 0.1 to 100 mg L⁻¹ for 1, 3 and 5 h. NPs coated with carboxylic (PS-COOH) and amine groups (PS-NH₂) were used to determine how surface properties influence the effects of nanoplastics. Results demonstrated the adhesion of NPs to oyster spermatozoa and oocytes as suggested by the increase of relative cell size and complexity measured by flow-cytometry and confirmed by microscopy observations. A significant increase of ROS production was observed in sperm cells upon exposure to 100 mg L⁻¹ PS-COOH, but was not observed with PS-NH₂, suggesting a differential effect according to the NP-associated functional group. Altogether, these results demonstrate that the effects of NPs occur rapidly, are complex and are possibly associated with the cellular eco-corona, which could modify NPs behaviour and toxicity.

Highlights

► Nanoplastics attach to both oocytes and spermatozoa. ► Cellular impacts of NPs was observed on spermatozoa. ► PS-COOH exposure generated a dose-response increase in ROS production in spermatozoa. ► Higher impact of PS-COOH suggest an influence of particle surface properties.

Keywords : Nanoplastics, Oysters, Gametes, Cellular responses

35 1. Introduction

36 Each year, more than 320 million tons of plastic are produced in the world (Plastic
37 Europe; 2016), and a large part of this finishes as waste in the oceans: an estimated 4.8–
38 12.7 million tons in 2010 (Jambeck et al., 2015). There is evidence of small particles of
39 plastic known as microplastics (MPs, <5mm) in global waters (Barnes et al., 2009).
40 However, because their identification is difficult, mainly due to limitations of
41 conventional sampling methods (sampling nets have a mesh size > 300 μm) and lack of
42 analytical techniques (Koelmans et al., 2015), little attention has been paid to smaller
43 particles of plastic known as nanoplastics (NPs) (GESAMP, 2016). Plastic particles are
44 considered *nano* in the strict sense, (i.e., defined in the same way as for non-polymer
45 nanomaterials in the field of engineered nanoparticles) if they are <100 nm in at least
46 two of their dimensions (Klaine et al., 2012; Koelmans et al., 2015). Nevertheless, the
47 NPs definition was enlarged to all polymeric particles <1000 nm (in at least one of its
48 dimensions) by the GESAMP (2016) because of their colloidal behaviour. Nanoplastics
49 can be found as part of many applications such as drug delivery, cosmetics, biosensors,
50 photonics, nanocomposites, paints, adhesives and coatings between others (Ganajan and
51 Tijare, 2018; Guterres et al. 2007; Hernandez et al., 2017; Merinska and Dujkova, 2012;
52 Rogach et al., 2000; Velev and Kaler, 1999). With the number of polymer applications
53 growing each year, it is estimated that, by 2020, NPs will account for most
54 nanomaterials on the market (Fabra et al., 2013) making the release of NPs by indirect
55 outputs an environmental concern. Small microplastics collected at sea have recently
56 been characterized (Ter Halle et al., 2017) and demonstrated to be increasingly
57 abundant following a power-law increase with decreasing particle size in sea surface
58 samples (Erni-Cassola et al., 2017).

59 Environmental effects of NPs are linked to their intrinsic features such as surface
60 charge, size, shape, functionalization and coating (Klaine et al., 2008). In addition, the
61 interaction of NPs with biological cells will be affected by their dispersion, aggregation
62 and agglomeration behaviour, which are dependent on the physico-chemical parameters
63 of the surrounding media (pH, temperature and ionic concentration) as well as the
64 presence/absence of natural colloids (Canesi et al., 2017). Thus, it is essential to
65 understand how NPs behave in the marine environment and how they interact with
66 marine organisms.

67 The Pacific oyster, *Crassostrea gigas*, has a worldwide distribution and has the highest
68 annual production of any aquatic organisms (around 630 000 tons registered worldwide
69 in 2014), far exceeding other molluscs (mussels, clams, cockles, etc.) (FAO statistics
70 data, 2016). During spawning, oysters release their gametes into the surrounding waters
71 where fertilization takes place. Consequently, oocytes and spermatozoa are very
72 vulnerable as they will be exposed to a wide range of environmental stressors present in
73 the surrounding water, notably pollutants including micro- and nano-sized plastics,
74 expected to be abundant in the water column (GESAMP, 2016). The effect of MPs on
75 these organisms has recently been published. Sussarellu et al., (2016) showed a
76 significant decrease of oocyte number and spermatozoa and oocyte quality upon
77 polystyrene microplastic exposure of adults during gametogenesis, leading to a negative
78 impact on D-larval yield and larval growth of experimental offspring. Working at early
79 development stages, Cole and Galloway (2015) showed that *C. gigas* larvae can readily
80 ingest small plastic particles (<20 μm) and internalized nano-sized plastics (<1 μm)
81 without any significant reported impacts. Both studies illustrated the ingestion of small
82 plastics by adults and early developmental stages. However, there is no information
83 available regarding the impact of small plastics, especially nano-sized plastics, on early

84 free living cells like oyster gametes. This is crucial information considering that the
85 quality of spermatozoa and oocytes is essential for successful fertilisation (Boulais et
86 al., 2015; 2017; Suquet et al., 2010). Upon spawning, fertilisation can occur within a
87 fairly long period (a few hours) as spermatozoa movement can be maintained up to 24 h
88 (Suquet et al., 2010) making this gametogenic phase very sensitive to waterborne
89 pollutants, especially in estuarine and coastal marine habitats. In these ecosystems,
90 environmental degradation is substantial, waters are greatly influenced by increased
91 human expansion, and we may expect peaks of nano-sized plastics close to industrial
92 sources, as already been observed for microplastics (Filella, 2015; Lambert and Wagner,
93 2016).

94 The objective of this study was to investigate interactions between polystyrene
95 nanoplastics and oyster gametes. Nanoplastics exhibiting different surface
96 functionalization with carboxylic groups (COOH) or primary amine (NH₂), as anionic
97 and cationic NPs, were used to assess the effects of particle surface properties, NPs
98 behaviour in seawater and ultimate toxicity. Due to the lack of information on
99 concentrations of nano-size particles in the environment, spermatozoa and oocytes were
100 exposed separately to a wide range of concentrations (0.1, 1, 10 and 100 mg L⁻¹ of PS-
101 NH₂ or PS-COOH) in order to identify a possible toxicity threshold. Nano-PS size,
102 charge and aggregation state in seawater and in oocyte and spermatozoa media were
103 monitored by Dynamic Light Scattering (DLS) during the experiment. Spermatozoa
104 motility and cellular responses of spermatozoa and oocytes in terms of viability, cellular
105 characteristics and Reactive Oxygen Species (ROS) production were monitored by flow
106 cytometry at 1, 3 and 5 h of NPs exposure.

107

108 **2. Materials and methods**

109 2.1. Measurements of nanoplastic characteristics

110 Fluorescent-green 100 nm amino (PS-NH₂) and carboxylic (PS-COOH) polystyrene
111 nanoparticles were purchased from Micromod laboratories (Germany) with an
112 Excitation/Emission: 475 nm/510 nm. To avoid commercial artefacts, nanobeads were
113 purchased from the same company and only differed in their functional groups. For
114 Dynamic Light Scattering analysis (DLS) the stock solutions (10 g L⁻¹) were diluted in
115 0.2- μ m filtered seawater (FSW) to a concentration of 100 mg L⁻¹. Size (Z-average),
116 charge and aggregation state (polydispersity index, PDI) of nanoplastics were
117 determined using a Zetasizer NanoZS (Malvern, United Kingdom). , in MilliQ water in
118 triplicate, each replicate corresponding to 13 runs for the Z-average and 40 runs for Z-
119 potential, following the protocol described in Della Torre et al. (2014). Data were
120 analyzed using Zetasizer Nano Series software, version 6.20. The nanoplastics were also
121 observed by transmission electronic microscopy (JeolJEM 100 CX II) to verify particle
122 size. In brief, nanoplastics were diluted in MilliQ (100 mg L⁻¹) and placed on a copper
123 grid (400 nm mesh) with a carbon-coated Formvar film (Polysciences) and marked with
124 2% (wt/vol) uranyl acetate to be measured.

125 To check the behaviour of NPs under experimental conditions, DLS measurements were
126 also performed on particles incubated in FSW and 0.2 μ m filtered seminal media in the
127 same conditions as those used during the experiment, i.e., kept in continuous movement
128 using a Stuart rotator SB3A. Filtered seminal media were prepared by filtering
129 spermatozoa (1×10^7 cells mL⁻¹ in FSW) and oocyte (2×10^5 cells mL⁻¹ in FSW) solutions
130 on a 0.2 μ m filter. Nano-PS concentration was adjusted to 100 mg L⁻¹ in both FSW and
131 seminal media. Measurements were performed after 1, 3 and 5 h using a Zetasizer Nano
132 as described above.

133 2.2. Gamete collection

134 Mature oysters from the north coast of Brittany (Aber Benoit: 48° 27' 31" N, 4° 20' 42"
135 W) were harvested and acclimated for 1 week before gamete collection in laboratory
136 conditions [1 µm filtered seawater, 18°C, continuous feeding on a mixed diet of two
137 microalgae *Chaetoceros gracilis* (UTEX LB2658), *T-Isochrysis* (clone: T-iso;
138 CCAP927/14)] to provide good physiological conditions prior spawning. The natural
139 seawater used for gamete resuspension and exposure to nanoplastics was UV-treated,
140 filtered at 0.2 µm and maintained at T = 18°C, salinity 38, pH 8.32 and conductivity 6
141 S/m.

142 Spermatozoa and oocytes were collected from individual males (n = 6; length: 110.9 ±
143 9.7 mm) and individual females (n = 6; length: 129.5 ± 8.9 mm) by stripping according
144 to Steele and Mulcahy (1999). Sperm motility was checked under a microscope. Final
145 concentration of 1×10^7 cells mL⁻¹ and 2×10^5 cells mL⁻¹ was adjusted with FSW for each
146 individual male and female, respectively.

147 2.3. Gamete exposure to nanoplastics

148 Oyster' gametes from males (n=6) and females (n=6) were individually exposed to NPs.
149 Four different concentrations of PS-COOH or PS-NH₂ were tested separately on oocytes
150 and spermatozoa: Control (no NPs), 0.1 , 1, 10 and 100 mg L⁻¹ of PS-COOH or PS-NH₂
151 which correspond to 0, 1.9×10^1 , 1.9×10^2 , 1.9×10^3 and 1.9×10^4 particles spermatozoa⁻¹;
152 and 1.9×10^3 , 1.9×10^4 , 1.9×10^5 and 1.9×10^6 particles oocyte⁻¹, respectively. Samples
153 were kept in continuous movement (program 3) using a Stuart rotator SB3 (Cole-
154 Parmer, UK) in order to prevent cell sedimentation, in a dark room at 18°C. Sampling
155 was performed in fresh samples after 1, 3 and 5 h exposure to NPs. Additionally, after

156 3h exposure, control and exposed samples of oocytes and spermatozoa were fixed in
157 formaldehyde (3% final) for later microscopy observations.

158 2.4. Analyses

159 2.4.1. Microscopy

160 2.4.1.1. Spermatozoa motility

161 To measure spermatozoa motility, fresh sperm solution was mixed with FSW
162 containing pluronic acid (PA 1g L⁻¹) (vol:vol) and transfer to a FastRead cell. The
163 percentage of motile spermatozoa, their movement linearity and velocity (VAP:
164 Velocity of the Average Path; $\mu\text{m sec}^{-1}$) were measured using CASA plug-in for the
165 Image J software adapted for Pacific oyster spermatozoa according to Suquet et al.
166 (2014) under a microscope (dark field, Olympus B×51, ×20 magnification), connected
167 to a video camera (Qicam Fast, 60 frames sec⁻¹).

168 2.4.1.2. Visualization of NP–gamete interactions

169 Once fixed in formaldehyde, both cell types emitted green fluorescence coming from
170 the fixative (formaldehyde). In order to better localize cells and discriminate the
171 fixative' green fluorescence from the diffuse green fluorescence of NPs, cell nucleus
172 were labelled in blue using DAPI ((4',6-diamidino-2-phenylindole), which emits blue
173 fluorescence upon binding to DNA. Cells were visualized using a confocal laser
174 scanning microscope Zeiss Axio Observer Z1 coupled to a ZEISS LSM780 confocal
175 laser module, with a Plan-Apochromat 63x/1.40 oil DIC M27 objective. Images were
176 made using two channels: ChS1-T1 (Ex/Em: 488/599 nm) and Ch1-T2 (Ex/Em:
177 405/449 nm). Images of spermatozoa 16.6 × 16.6 μm in size (X-scaling × Y-scaling)
178 were acquired at a sampling speed of 6.7 $\mu\text{s}/\text{pixel}$ and a zoom of 8.1. Images of oocytes
179 112.4 × 112.4 μm in size (X-scaling × Y-scaling) were acquired at a sampling speed of

180 1.8 $\mu\text{s}/\text{pixel}$ and a zoom of 1.2. The images were obtained using ZEN 2012 SP2
181 software (Carl Zeiss Microscopy GmbH, Germany).

182 2.4.2. Flow cytometry

183 Analyses were performed using an EasyCyte Plus cytometer (Guava Technologies,
184 Millipore, Billerica, MA), equipped with a 488-nm argon laser and three fluorescence
185 detectors: green (525/30 nm), yellow (583/26 nm) and red (680/30 nm). Flow cytometry
186 analysis were performed in fresh samples with or without fluorescent probes as
187 described below. To run the different tests, cytometer' setting were established using
188 unlabelled cell population (negative control) for which was assigned a relative (low) but
189 non-zero fluorescence value.

190 2.4.2.1. Cell number, relative size and complexity

191 Spermatozoa and oocyte cell numbers were recorded in fresh samples without adding
192 fluorescent probe with and without NPs, over 30 sec at $0.12 \mu\text{L sec}^{-1}$ flow rate for
193 spermatozoa and at $0.59 \mu\text{L sec}^{-1}$ for oocytes. Cells were detected and described on the
194 flow-cytometer according to their optical characteristics obtained at small angle
195 (Forward Scatter: FSC) and large angle (Side Scatter: SSC) giving respectively
196 information on relative size and complexity of cells. For analysis of sperm samples, two
197 regions were designed to discriminate single and aggregate spermatozoa.

198 2.4.2.2. Cell mortality

199 Viability was measured after 10 minutes of incubation with SYBR-14 for spermatozoa
200 and SYBR-green for oocytes (final concentration: 1/100 commercial solution) together
201 with propidium iodide (PI, final concentration: 10mg L^{-1}) following the protocols
202 established by Le Goïc et al. (2013; 2014) for spermatozoa and oocytes, respectively. PI
203 penetrates cells that have lost membrane integrity and are considered to be dead
204 (orange/red fluorescence), whereas SYBR-green, which binds DNA, penetrates both

205 dead and living oocytes (green fluorescence, SYBRgreen fluorescence later in the text)
206 and SYBR-14 binds DNA of live spermatozoa only. The percentage of dead oocytes
207 and spermatozoa was calculated by the ratio between the number of cells showing
208 orange/red fluorescence (PI) and the total number of cells $\times 100$. Results were
209 expressed as percentages of dead cells.

210 A strong decrease in viability was observed in control oocytes at 5 h incubation, which
211 is consistent with the short life cycle of oocytes. In consequence, after 5 h exposure all
212 samples of oocytes were excluded from the data.

213 *2.4.2.3. Reactive Oxygen Species (ROS) production*

214 ROS production by cells was measured using 2,7-dichlorofluorescein diacetate (DCFH-
215 DA) after 50 min of incubation at 18°C. DCFH is hydrolysed (esterase) intracellularly to
216 form DCF, which turns fluorescent green upon oxidation with ROS. The green
217 fluorescence measured is quantitatively related to the ROS production in cells and was
218 expressed in arbitrary units (A.U.).

219 *2.3.2.4. Flow cytometry data normalization*

220 After exposure to both NPs, green fluorescence level of unlabelled cells were higher in
221 the presence of nanoparticles (exposed cells) than in their absence (control cells). Thus,
222 fluorescence values of negative controls from both, spermatozoa and oocytes, were
223 subtracted from the labelled cells' fluorescence data obtained after addition of the
224 different fluorescent probes: DCFH-DA (ROS production) and SYBRgreen/SYBR14
225 (viability). This was done to avoid any bias due to an increase in the cells' background
226 green fluorescence observed during PS-COOH and PS-NH₂ exposure.

227

228 *2.5 Statistical analyses*

229 Statistical analyses were performed using STATGRAPHICS Centurion XVII and were
230 carried out separately for PS-COOH and PS-NH₂ conditions treatments. When the
231 requirements of normality and homogeneity of variances were met, one-way ANOVAs
232 were performed to establish significant differences between treatments at each sampling
233 time. Tukey's post-hoc test was used to test for differences among the different
234 exposure treatments with $P < 0.05$ as the significance level for all analyses. Arcsine or
235 log transformation was performed when necessary to meet the normality and
236 homoscedasticity criteria. Non-parametric analysis (Kruskal-Wallis test) was performed
237 when the variables did not meet the requirements of ANOVA. In addition, simple
238 regressions using the coefficient of determination (R^2) were used to investigate the
239 relationship between spermatozoa motility parameters and ROS production, with $P <$
240 0.05 as the significance level for all analyses.

241

242 **3. Results**

243 3.1. Nanoplastic size, charge and aggregation under experimental conditions

244 DLS analysis confirmed the outlined size of NPs in MilliQ water, with a Z-average of
245 131.82 ± 0.23 nm (mean \pm SD) and 130.83 ± 0.32 nm, for PS-COOH and PS-NH₂,
246 respectively (Figure 1A-B). The expected size of NPs was also observed in FSW with
247 140.11 ± 0.92 nm and 141.13 ± 1.50 nm for PS-COOH and PS-NH₂, respectively.
248 Aggregation was negligible as suggested by a PDI < 0.2 for both particle types in MilliQ
249 and FSW conditions. Nanoparticle geometric diameter was also confirmed using
250 transmission electron microscopy (Fig. 1C-D).

251 Results of NPs size and aggregation state monitored under constant rotation (to
252 reproduce the incubation conditions) in FSW and in seminal media did not show any

253 changes in size or aggregation, regardless of the particle type, media or incubation time
254 (PdI < 0.2).

255 Both NPs resuspended in FSW showed a negative charge: -2.89 ± 7.21 mV and $-5.69 \pm$
256 3.65 mV for PS-COOH and PS-NH₂, respectively. Similar behaviour was observed in
257 oocyte and spermatozoa media, with charges of -8.17 ± 4.66 and -13.60 ± 2.92 for PS-
258 COOH and values of -8.26 ± 3.20 and -6.95 ± 1.37 mV for PS-NH₂, respectively.

259 3.2. Visualization of interactions between NPs and oyster gametes

260 Images of spermatozoa and oocytes exposed to the highest concentration of PS-COOH
261 are shown in Figure 2 alongside the controls. Only particles displaying significant
262 biological effects (PS-COOH) were measured by microscopy. In order to localize
263 cellular structures and discriminate from fixative' fluorescence (green also) and
264 nanoplastics' fluorescence (green), cells were labelled with DAPI which allow staining
265 nucleus DNA in blue (Fig. 2A; 2B). As a result, it was possible to localize NPs
266 aggregates attached to the cells (Fig. 2C and 2D). In spermatozoa, aggregates of NPs
267 were found attached mainly to the acrosome (Fig. 2C). Interaction of NPs with oocytes
268 is shown in Fig. 2D, with oocytes covered by a semi-transparent structure formed by
269 colloids and debris present in the medium. The aggregates of NPs appeared to be
270 entrapped inside this structure and not directly attached to the cell.

271 3.3. Cellular responses of gametes exposed to NPs

272 3.3.1 *Cell number, relative size and complexity*

273 After 3 h and 5 h of exposure to 100 mg L^{-1} PS-COOH, a significant decrease in the
274 number of single spermatozoa was observed: 32% and 24% lower than the control (P
275 <0.01 and P <0.05), respectively. This decrease was directly correlated with the increase

276 in spermatozoa' aggregates for this NP condition ($P < 0.05$ and $P < 0.01$ after 3h and 5h
277 exposure to 100 mg L^{-1} PS-COOH). No significant formation of spermatozoa'
278 aggregates was observed in treatments exposed to PS-NH₂, and consequently, no
279 differences in single spermatozoa number was reported. Spermatozoa exposed to the
280 highest concentration of PS-COOH and PS-NH₂ showed a 4-5% increase in relative size
281 compared with controls after 1, 3 and 5 h exposure. Spermatozoa also showed higher
282 cellular relative complexity upon exposure to 10 and 100 mg L^{-1} . An increase of 24%,
283 25% and 25% cellular complexity at 10 mg L^{-1} and 53%, 24% and 52% increase at 100
284 mg L^{-1} was observed after 1, 3 and 5 h exposure to PS-COOH. Similar tendency was
285 observed upon exposure to PS-NH₂ that revealed a 14%, 15% and 19 % increase at 10
286 mg L^{-1} whereas increased values of 59%, 37% and 62% were observed at 100 mg L^{-1}
287 after 1, 3 and 5 h exposure, respectively. By contrast, no significant changes in oocyte
288 cell number, relative size or complexity were observed by flow cytometry in the whole
289 experiment.

290 3.3.2 Cell mortality

291 After exposure to the highest NP concentration (100 mg L^{-1}), oocytes exposed to both
292 NPs types showed a decrease in their SYBRgreen fluorescent signal for both exposure
293 times 1 and 3 h ($P < 0.001$ and $P < 0.01$ for PS-COOH and PS-NH₂, respectively at both
294 time points). Due to the significant decrease of SYBRgreen fluorescent observed in all
295 females (e.g: Supplementary figure 1 for one female), fluorescent value of PI cannot be
296 considered either. Thus, viability test for this NP condition is not conclusive and cannot
297 be considered. For the other 3 NP exposures (0.1 , 1 and 10 mg L^{-1}) where the values of
298 SYBRgreen and PI fluorescence were validated, no significant differences in the
299 percentage of dead cells were observed in exposed oocytes regardless of exposure
300 duration.

301 No significant differences were observed in the percentage of dead cells in spermatozoa
302 exposed to NPs among sampling times (from 1 to 5 h exposure) for none of the tested
303 NPs.

304 3.3.3 ROS production

305 Control spermatozoa showed 17.1 ± 5.7 (CV=33.8), 24.3 ± 8.2 (CV=33.7) and $22.4 \pm$
306 9.7 (CV=43.55) A.U. of ROS production at 1, 3 and 5 h, respectively. After 1 h of
307 exposure to PS-COOH, a dose-response increase in ROS production was observed in
308 spermatozoa exposed to 1, 10 and 100 mg L^{-1} ($P < 0.001$) that was 17.4%, 59.4% and
309 121% higher respectively than in the control. After 3 and 5 h, significant increases were
310 only observed in spermatozoa exposed to 10 and 100 mg L^{-1} ($P < 0.001$ and $P < 0.01$ for
311 3 and 5 h, respectively) with ROS values around 30% and 70% higher than in control
312 (Figure 3). Spermatozoa exposed to PS-NH₂ were not significantly affected.

313 ROS production in oocytes was not significantly affected by NP exposure. Levels of
314 ROS production in control oocytes ranged from 8.7 to 44.3 A.U. (24.9 ± 11.2 A.U.; CV
315 = 121.5 and 20.6 ± 12.8 A.U.; CV = 126.3 after 1 and 3 h of incubation, respectively)
316 showing a high inter-individual variability in stress response.

317 3.3.4. Spermatozoa motility

318 No significant differences were observed in the percentage of motile spermatozoa, VAP
319 or movement linearity after exposure to NPs. Nevertheless, when spermatozoa were
320 exposed to PS-COOH, a significantly positive correlation was found between the
321 percentage of motile spermatozoa and spermatozoa' ROS production through the
322 experiment ($R^2 = 0.12$, $P < 0.001$), particularly after 5 h exposure ($R^2 = 0.24$, $P < 0.001$).

323

324 **4. Discussion**325 **Nanoplastics had similar size and charge in seawater and seminal media over time**

326 The most important feature of nanoplastics is their high surface area-to-volume ratio
327 (Mattsson et al., 2015), which makes them highly reactive and prone to strongly interact
328 with biological membranes (Rossi et al., 2014). In general, nanoplastics, as hydrophobic
329 particles, are not thermodynamically stable and tend to aggregate very easily, forming
330 agglomerates. However, they can become soluble if they are charged since electrostatic
331 repulsions fight against attractive van der Waals forces as explained by the classic
332 Derjaguin–Landau–Verwey–Overbeek (DLVO) theory (Derjaguin, 1941; Verwey et al.,
333 1999). In the present work, oyster gametes were exposed to free single NPs of 100 nm,
334 as nanoplastics did not aggregate in seawater or seminal media over time. Our results
335 are in agreement with Cai et al. (2018) which recently reported absence of aggregation
336 in 100 nm polystyrene nanoplastics in NaCl and CaCl₂ solutions charged with humic
337 substances. This behaviour was explained by the fact that electrostatic repulsive forces
338 increased in presence of organic matter in these solutions. Nevertheless, Cai and co-
339 authors highlighted that aggregation behaviour of nanoplastics is influenced by complex
340 environmental factors and further research is necessary to understand these interactions.

341 In the present study, a higher impact was observed with PS-COOH than with PS-NH₂,
342 contrary to previous works which revealed a higher impact of positively charged nano-
343 polystyrene particles on different marine organisms: Crustacea (Bergami et al., 2016 ;
344 2017 ; Nasser and Lynch, 2016) Bivalvia (Balbi et al., 2017) Equinodea (Della Torre et
345 al., 2014) and Chlorophyceae (Bergami et al., 2017). Positively-charged NPs have been
346 suggested to interact more strongly with biological membranes, as demonstrated by *in*
347 *vitro* studies with mammalian cells (Anguissola et al., 2014; Varela et al., 2012). In the

348 present study, both PS-COOH and PS-NH₂ showed negative charges when they were
349 suspended in seawater. Changes on nanoplastics charge is not surprising as, once in
350 seawater, NPs can interact rapidly with the high number of charged ions (H⁺ and OH⁻)
351 present (Cole and Galloway, 2015). Additionally, in natural environments, NPs can
352 interact with natural colloids, sediment and soils, forming an *eco-corona* coating that
353 potentially affects the fate of NPs in the water column, bioavailability, toxicity and
354 uptake (Canesi et al., 2017; Galloway et al., 2017). Afshinnia et al. (2018) reported that
355 natural colloids from the media (e.g., humic substances) inverted the charge in silver
356 nanoparticles (AgNPs), suppressing the positive charge and enhancing the negative one,
357 depending on point zero charge of the particles and the solution pH. Nevertheless,
358 positive charges of 50 nm polystyrene amino coated (PS-NH₂) in seawater has been
359 reported in other studies (Bergami et al., 2017; Della Torre et al., 2014; Manfra et al.,
360 2017). This obliges us to ask whether the size or the commercial supplier has an impact
361 on particles characteristics in seawater. More information about physico-chemical
362 characteristics of nanoplastics is needed for better interpretation of NPs behavior in
363 different solutions. In addition, more powerful techniques should be used considering
364 the limitations of DLS technique which, according to ZETASIZER manual, cannot
365 provide accurate Z-potential between -10 to +10 mV. Overall, in our study, NPs were
366 from the same commercial brand and size, differing only in coated functional group and
367 charge. As consequence, the differences in toxicity observed between PS-COOH and
368 PS-NH₂ are probably not related to the size, aggregation state or even charge of the
369 particles, which were similar between the two particle types. Instead, the nature of the
370 coating (carboxylic or amine) may have interacted differently with the cell membranes,
371 either directly or through interaction with specific biomolecules present in each seminal
372 medium.

373 **Nanoplastics attachment to spermatozoa and micro-scale aggregate formation**
374 **around oocytes**

375 Spermatozoa consist of a head (between 2–3 μm length), which contains the acrosome,
376 an intermediate part and the flagellum ($\sim 33 \mu\text{m}$ in mature spermatozoa) (Demoy-
377 Schneider et al., 2013). The increase in relative size and complexity observed upon
378 exposure to NPs is likely explained by an adhesion of NPs mostly to the spermatozoa
379 head, as observed for PS-COOH using confocal microscopy. Similarly, an increase in
380 relative size and relative complexity of algal cells was previously reported under
381 exposure to metallic nanoparticles, but the localization of these particles was not
382 confirmed by microscopy (Sendra et al., 2017).

383 Regarding the oocytes, NPs formed hetero-aggregates with the organic matter from
384 seminal media that were entrapped to the cells. These aggregates were not present in all
385 observations, which is probably due to the high variability observed in cell responses to
386 NP exposure. Also as microscopy observations were performed on fixed samples,
387 addition of fixative could have led to modifications regarding NPs adhesion.
388 Nevertheless, slight modifications are expected since fixative was added after exposure
389 of oocytes to NPs.

390 **Nanoplastics exposure affects spermatozoa more than oocytes**

391 Differential effects of NPs observed between spermatozoa and oocytes could be
392 explained by differences in their membrane characteristics (Kline, 1991). In our study,
393 we observed NPs attached to both, spermatozoa and oocytes. NPs exposure favour
394 spermatozoa aggregation on the PS-COOH conditions. The increase of spermatozoa
395 aggregates was concomitant to the decrease of single spermatozoa cell number observed
396 upon exposure to PS-COOH. Conversely, no aggregation was observed in oocytes.

397 Oocytes appeared to be covered by a transparent structure, probably from the molecules
398 and colloids present in the medium that were absent from the spermatozoa samples. In
399 general, the presence of proteins reduces the free energy of the NP surface, thus
400 reducing unspecific adhesion to the membrane (Lesniak et al., 2013). Gao et al. (2017)
401 recently reported sex-specific differences in the protein composition of the nanoparticle
402 corona in fish and suggested that some specific proteins related to vitellogenin coated
403 nanoparticles in developing oocytes. Such a mechanism may explain why, in our study,
404 we observed a differential interaction of NPs between spermatozoa and oocytes. Other
405 factors such as (i) the high inter-individual variability in oocyte quality, as previously
406 observed for this species (Boudry et al., 2002), potentially masking the effects of NPs,
407 (ii) the way the oocytes were collected, i.e., because the gonads were stripped, the
408 samples would have included potentially immature oocytes (Le Goïc et al., 2014), or
409 (iii) natural characteristics of each cell type such as the size, 40 times higher oocytes
410 than spermatozoa and functional structures (spermatozoa with a motile flagella vs
411 oocytes not motile and with higher lipid content) could explain the difference in NPs
412 effects between spermatozoa and oocytes.

413 During the viability test in oocytes, NPs exposure (100 mg L^{-1}) promote a significant
414 decrease of SYBRgreen fluorescence after exposure to both PS-COOH and PS-NH₂.
415 This effect may be likewise caused by several factors (i) interaction of NPs with the
416 fluorescent dye (SYBRgreen), (ii) a reduction in DNA content related to chromosome
417 anomalies or chromosome deletions (Haberkorn et al., 2010), or even (iii) changes in
418 the membrane permeability which may also impair the entry or retention of the
419 SYBRgreen into the cells. Cellular membrane hyperpolarization has been demonstrated
420 in other organisms after exposure to pollutants (Seoane et al., 2017). Unfortunately,
421 Pacific oyster oocyte ultrastructure remains poorly described and its envelope thickness

422 is not precisely known (Suquet, et al., 2007), which hinders a thorough understanding
423 of the biological response observed in exposed gametes in this work. Further research is
424 needed to explore the interaction between NPs and gamete membranes in greater depth,
425 which will require challenging technological developments in microscope visualization.

426 **Increase in ROS production by spermatozoa upon exposure to PS-COOH**

427 The dose-response generation of intracellular ROS observed in spermatozoa exposed to
428 PS-COOH calls into question their subsequent ability to fertilize oocytes. Increase in
429 ROS production and oxidative damage upon exposure to micro- and nanoplastics has
430 been observed in other species, such as the lugworm (*Arenicola marina*; Browne et al.,
431 2013), a planktonic crustacean (*Daphia magna*; Ma et al., 2016; Nasser and Lynch,
432 2016), algae (*Chlorella* and *Scenedesmus*; Bhattacharya et al., 2010), mussels (*Mytilus*
433 spp.; Paul-Pont et al., 2016) and zebrafish larvae (*Danio rerio*; Chen et al., 2017). ROS
434 generation and the subsequent oxidative stress have been described as the predominant
435 mechanism leading to nano-toxicity, including DNA damage, unregulated cell
436 signalling, changes in cell motility, cytotoxicity, apoptosis and cancer initiation and
437 promotion (Fu et al., 2014). However, in the present study, the increase in ROS did not
438 lead to any effects on cell motility or viability, suggesting that the oxidative stress
439 produced was not sufficient to cause irreversible damage. From another perspective,
440 ROS play important roles in spermatozoa physiological functions in different species
441 including capacitation, hyperactivation and the acrosome reaction (Kothari et al., 2010;
442 Zilli and Schiavone, 2016 in Aitken, 2017). In the present study, the positive correlation
443 observed between the percentage of motile spermatozoa and their ROS production after
444 being exposed to PS-COOH, particularly after 5 h exposure, may suggest the
445 stimulation of spermatozoa capacitation as previously reported in mammals after an
446 increase in intracellular ROS content (Aitken, 2017). Nevertheless, when ROS

447 production overcomes the oxidative balance of spermatozoa, a decrease in spermatozoa
448 motility may occur as it has been reported in other studies carried out with mouse sperm
449 exposed to metallic nanoparticles (Hong et al., 2015; Kumar et al., 2001). Further
450 studies using biochemical markers of oxidative stress (MDA formation, lipid
451 peroxidation, etc.) would be useful to clarify the impacts of ROS production induced by
452 NP exposure observed here.

453 **5. Conclusion**

454 The present study evaluated the effects of nanoplastics on oyster gametes that are in
455 close contact with water-borne pollution and thus constitute very sensitive life stages.
456 Our results demonstrated adhesion of NPs to oyster spermatozoa leading to an increase
457 in relative cell size and complexity. A significant dose-response increase in ROS
458 production by spermatozoa was demonstrated upon exposure to PS-COOH, but not with
459 PS-NH₂. Conversely, oocytes were less impacted after exposure to both NPs.

460 Differences in effects between the NPs and the two gamete cells were not related to
461 particle size, charge or aggregation state, as tested NPs displayed similar features over
462 time both in seawater and seminal media. Instead, results suggest that interactions with
463 seminal biomolecules and/or cell membranes differed according to particle coating and
464 gametes' type. It would be of further interest to investigate the nature of the eco-corona
465 formed on nanoplastics and how this modifies particle toxicity toward oyster gametes.
466 Subsequent impacts of gamete exposure to NPs on oyster reproductive success could be
467 assessed by studying the fertilization rate as proxy of gamete quality (Boulais et al.
468 2015), as well as embryo-larval development.

469 **Acknowledgements**

470 The authors thank the staff of the Ifremer facilities in Argenton. We are particularly
471 grateful to Dr. Philippe Elies from the PIMM core facilities and Olivier Lozach from the
472 COSM team at the University of Western Brittany for the microscopy observations and
473 DLS measurements. This work was supported by the NANO Project (ANR-15-CE34-
474 0006-02) funded by the French *Agence Nationale de la Recherche* (ANR). We thank
475 Helen McCombie for their help in editing the English. K. Tallec was funded by a
476 French doctoral research grant from Ifremer (50%) and Region Bretagne (50%).

477 **References**

478 Aitken, R.J., 2017. Reactive oxygen species as mediators of sperm capacitation and
479 pathological damage. *Mol. Reprod. Dev.* 84, 1039–1052.
480 <https://doi.org/10.1002/mrd.22871>

481 Anguissola, S., Garry, D., Salvati, A., O'Brien, P.J., Dawson, K.A., 2014. High content
482 analysis provides mechanistic insights on the pathways of toxicity induced by amine-
483 modified polystyrene nanoparticles. *PLoS One* 9.
484 <https://doi.org/10.1371/journal.pone.0108025>

485 Afshinnia, K., Marrone, B., Baalousha, M., 2018. Potential impact of natural organic
486 ligands on the colloidal stability of silver nanoparticles. *Sci. Total Environ.* 625, 1518–
487 1526. <https://doi.org/10.1016/j.scitotenv.2017.12.299>

488 Balbi, T., Camisassi, G., Montagna, M., Fabbri, R., Franzellitti, S., Carbone, C.,
489 Dawson, K., Canesi, L., 2017. Impact of cationic polystyrene nanoparticles (PS-NH₂)
490 on early embryo development of *Mytilus galloprovincialis*: Effects on shell formation.
491 *Chemosphere* 186, 1–9. <https://doi.org/10.1016/j.chemosphere.2017.07.120>

- 492 Barnes, D.K.a., Galgani, F., Thompson, R.C., Barlaz, M., 2009. Accumulation and
493 fragmentation of plastic debris in global environments. *Philos. Trans. R. Soc. Lond. Ser.*
494 *B Biol. Sci.* 364 (1526), 1985–1998.
- 495 Bhattacharya, P., Lin, S., Turner, J.P., Ke, P.C., 2010. Physical adsorption of charged
496 plastic nanoparticles affects algal photosynthesis. *J. Phys. Chem. C* 114, 16556–16561.
497 <https://doi.org/10.1021/jp1054759>
- 498 Bergami, E., Bocci, E., Vannuccini, M.L., Monopoli, M., Salvati, A., Dawson, K.A.,
499 Corsi, I., Luisa, M., Monopoli, M., Salvati, A., Dawson, K.A., Corsi, I., 2016. Nano-
500 sized polystyrene affects feeding, behavior and physiology of brine shrimp *Artemia*
501 *franciscana* larvae. *Ecotoxicol. Environ. Saf.* 123, 18–25.
502 <https://doi.org/10.1016/j.ecoenv.2015.09.021>
- 503 Bergami, E., Pugnali, S., Vannuccini, M.L., Manfra, L., Faleri, C., Savorelli, F.,
504 Dawson, K.A., Corsi, I., 2017. Long-term toxicity of surface-charged polystyrene
505 nanoplastics to marine planktonic species *Dunaliella tertiolecta* and *Artemia*
506 *franciscana*. *Aquat. Toxicol.* 189, 159–169.
507 <https://doi.org/10.1016/j.aquatox.2017.06.008>
- 508 Boudry, P., Collet, B., Cornette, F., Hervouet, V., Bonhomme, F., 2002. High variance
509 in reproductive success of the Pacific oyster (*Crassostrea gigas*, Thunberg) revealed by
510 microsatellite-based parentage analysis of multifactorial crosses. *Aquaculture* 204, 283–
511 296. doi:10.1016/S0044-8486(01)00841-9
- 512 Boulais, M., Corporeau, C., Huvet, A., Bernard, I., Quéré, C., Quillien, V., Fabioux, C.,
513 and Suquet, M. 2015. Assessment of oocyte and trochophore quality in Pacific oyster,
514 *Crassostrea gigas*. *Aquaculture* 437, 201–207.
515 <https://doi.org/10.1016/j.aquaculture.2014.11.025>

- 516 Boulais, M., Soudant, P., Le Goïc, N., Quéré, C., Boudry, P., Suquet, M., 2017. ATP
517 content and viability of spermatozoa drive variability of fertilization success in the
518 Pacific oyster (*Crassostrea gigas*). *Aquaculture* 479, 114–119.
519 <https://doi.org/10.1016/j.aquaculture.2017.05.035>
- 520 Browne, M.A., Niven, S.J., Galloway, T.S., Rowland, S.J., Thompson, R.C., 2013.
521 Report Microplastic Moves Pollutants and Additives to Worms , Reducing Functions
522 Linked to Health and Biodiversity. *CURBIO* 23, 2388–2392.
523 <https://doi.org/10.1016/j.cub.2013.10.012>
- 524 Cai, L., Hu, L., Shi, H., Ye, J., Zhang, Y., Kim, H., 2018. Effects of inorganic ions and
525 natural organic matter on the aggregation of nanoplastics, *Chemosphere*. 197:142-151.
526 <https://doi.org/10.1016/j.chemosphere.2018.01.052>
- 527 Canesi, L., Balbi, T., Fabbri, R., Salis, A., Damonte, G., Volland, M., Blasco, J., 2017.
528 Biomolecular coronas in invertebrate species: Implications in the environmental impact
529 of nanoparticles. *NanoImpact* 8, 89–98. <https://doi.org/10.1016/j.impact.2017.08.001>
- 530 Chen, Q., Gundlach, M., Yang, S., Jiang, J., Velki, M., Yin, D., Hollert, H., 2017.
531 Quantitative investigation of the mechanisms of microplastics and nanoplastics toward
532 zebrafish larvae locomotor activity. *Sci. Total Environ.* 585, 1022–1031.
533 [doi:10.1016/j.scitotenv.2017.01.156](https://doi.org/10.1016/j.scitotenv.2017.01.156)
- 534 Cole, M., Galloway, T.S., 2015. Ingestion of Nanoplastics and Microplastics by Pacific
535 Oyster Larvae. *Environ. Sci. Technol.* 49, 14625–14632.
536 <https://doi.org/10.1021/acs.est.5b04099>
- 537 Della Torre, C., Bergami, E., Salvati, A., Faleri, C., Cirino, P., Dawson, K.A., Corsi, I.,
538 2014. Accumulation and Embryotoxicity of Polystyrene Nanoparticles at Early Stage of

- 539 Development of Sea Urchin Embryos *Paracentrotus lividus*. Environ. Sci. Technol. 48,
540 12302–12311. <https://doi.org/10.1021/es502569w>
- 541 Demoy-Schneider, M., Schmitt, N., Suquet, M., Labbé, C., Boulais, M., Prokopchuk,
542 G., Cosson, J., 2013. Biological characteristics of sperm in two oyster species: the
543 Pacific oyster, *Crassostrea gigas*, and the blacklip pearl oyster, *Pinctada margaritifera*.
544 In “Spermatozoa: Biology, Motility and Function and Chromosomal abnormalities”,
545 Chapter 2, Nova Science Publishers Inc., Brenda T. Erickson Editor, ISBN: 978-1-63, p.
546 15-74
- 547 Derjaguin, B. V. 1941. Theory of the stability of strongly charged lyophobic sols and
548 the adhesion of strongly charged particles in solutions of electrolytes. Acta. Physiochim.
549 URS. 14, 633-662.
- 550 Erni-Cassola, G., Gibson, M.I., Thompson, R.C., christie-oleza, J., 2017. Lost, but
551 found with Nile red; a novel method to detect and quantify small microplastics (20 µm–
552 1 mm) in environmental samples. Environ. Sci. Technol., 2017, 51 (23), 13641–13648
- 553 FAO. 2016. The State of World Fisheries and Aquaculture 2016. Contributing to food
554 security and nutrition for all. Rome. 200 pp.
- 555 Fabra, M.J., Busolo, M.A., Lopez-Rubio, A., Lagaron, J.M., 2013. Nanostructured
556 bilayers in food packaging. Trends Food Sci. Technol. 31, 79–87.
- 557 Filella, M. 2015. Questions of size and numbers in environmental research on
558 microplastics: methodological and conceptual aspects. Environ Chem 12:527.
- 559 Fu, P.P., Xia, Q., Hwang, H., Ray, P.C., 2014. Mechanisms of nanotoxicity : Generation
560 of reactive oxygen species. J. Food Drug Anal. 22, 64–75.
561 <https://doi.org/10.1016/j.jfda.2014.01.005>

- 562 Gajanan, K, Tijare, N., 2018. Nanomaterials applications. *Proceedings*. 5, 1093–1096.
- 563 Gao, J., Lin, L., Wei, A., Sepúlveda, M.S., 2017. Protein corona analysis of silver nano-
564 particles exposed to fish plasma. *Environ. Sci. Technol. Lett.* 4, 174–179.
- 565 Galloway, T.S., Cole, M., Lewis, C., 2017. Interactions of microplastic debris
566 throughout the marine ecosystem. *Nat. Ecol. Evol.* 1, 1-16.
567 <https://doi.org/10.1038/s41559-017-0116>
- 568 GESAMP. 2016. “Sources, fate and effects of microplastics in the marine environment:
569 part two of a global assessment” (Kershaw, P.J., and Rochman, C.M., eds).
570 (IMO/FAO/UNESCO-IOC/UNIDO/WMO/IAEA/UN/UNEP/UNDP Joint Group of
571 Experts on the Scientific Aspects of Marine Environmental Protection). Rep. Stud.
572 GESAMP No. 93, 220 p.
- 573 Guterres, S. S., Marta, P. A., & Adriana, R. P. 2007. Polymeric nanoparticles,
574 nanospheres and nanocapsules, for cutaneous applications. *Drug Target Insights*, 2,
575 147–157
- 576 Haberkorn, H., Lambert, C., Le Goïc, N., Moal, J., Suquet, M., Guéguen, M., Sunila, I.,
577 Soudant, P., 2010. Effects of *Alexandrium minutum* exposure on nutrition-related
578 processes and reproductive output in oysters *Crassostrea gigas*. *Harmful Algae* 9, 427–
579 439. <https://doi.org/10.1016/j.hal.2010.01.003>
- 580 Hernandez, L. M., Yousefi, N., & Tufenkji, N. 2017. Are There Nanoplastics in Your
581 Personal Care Products? *Environ Sci Technol Lett.* 4(7), 280–285.
582 <https://doi.org/10.1021/acs.estlett.7b00187>
- 583 Hong, F., Zhao, X., Si, W., Ze, Y., Wang, L., Zhou, Y., Hong, J., Yu, X., Sheng, L.,
584 Liu, D., Xu, B., Zhang, J., 2015. Decreased spermatogenesis led to alterations of testis-

- 585 specific gene expression in male mice following nano-TiO₂ exposure. *J. Hazard. Mater.*
586 300, 718–728. <https://doi.org/10.1016/j.jhazmat.2015.08.010>
- 587 Jambeck, J. R., Geyer, R., Wilcox, C., Siegler, T. R., Perryman, M., Andrady, A.,
588 Narayan, R., Law, K. L. 2015. Plastic waste inputs from land into the ocean. *Science*,
589 347(6223), 768–771
- 590 Klaine, S.J., Alvarez, P.J.J., Batley, G.E., Fernandes, T.F., Handy, R.D., Lyon, D.Y.,
591 Mahendra, S., McLaughlin, M.J., Lead, J.R., 2008. Nanomaterials in the environment:
592 behavior, fate, bioavailability, and effects. *Environ. Toxicol. Chem.* 27 (9), 1825–1851
- 593 Klaine, S. J., Koelmans, A. A., Horne, N., Handy, R. D., Kapustka, L., Nowack, B., &
594 von der Kammer, F. (2012). Paradigms to assess the environmental impact of
595 manufactured nanomaterials. *Environmental Toxicology and Chemistry*, 31, 3–14.
- 596 Kline, D. 1991. Developmental Biology of membrane Transport Systems, in: Benos,
597 D.J (Eds.), *Current topics in membranes*. ISBN:978-0-12-1533339-7, Vol 39, pp. 3-394.
- 598 Koelmans, A.A., Besseling, E., Shim, W.J., 2015. Nanoplastics in the aquatic
599 environment. In: Bergmann, M., Gutow, L., Klages, M. (Eds.), *Marine Anthropogenic*
600 *Litter*. Springer, Berlin, pp. 329–344.
- 601 Kothari, S., Thompson, A., Agarwal, A., Plessis, S.S. du, 2010. Free radicals : Their
602 beneficial and detrimental effects on sperm function. *IJEB* Vol4805 May 2010.
- 603 Kumar, T., Doreswamy, K., Shrilatha, B., Muralidhara, B. 2001. Oxidative stress
604 associated DNA damage in testis of mice: Induction of abnormal sperms and effects on
605 fertility. *Mutat. Res. Genet. Toxicol. Environ. Mutagen.* 513, 103–111.
606 [https://doi.org/10.1016/S1383-5718\(01\)00300-X](https://doi.org/10.1016/S1383-5718(01)00300-X)

- 607 Lambert, S., Wagner, M., 2016. Characterisation of nanoplastics during the degradation
608 of polystyrene. *Chemosphere* 145, 265–268.
609 <https://doi.org/10.1016/j.chemosphere.2015.11.078>
- 610 Le Goïc, N., Hégaret, H., Fabioux, C., Miner, P., Suquet, M., Lambert, C., Soudant,
611 2013. Impact of the toxic dinoflagellate *Alexandrium catenella* on Pacific oyster
612 reproductive output: application of flow cytometry assays on spermatozoa. *Aquat.*
613 *Living Resour.* 26, 221–228. <https://doi.org/10.1051/alr/2013047>
- 614 Le Goïc, N., Hégaret, H., Boulais, M., Béguel, J.P., Lambert, C., Fabioux, C., Soudant,
615 P., 2014. Flow cytometric assessment of morphology, viability, and production of
616 reactive oxygen species of *Crassostrea gigas* oocytes. Application to Toxic
617 dinoflagellate (*Alexandrium minutum*) exposure. *Cytometry A* 85, 1049–1056. doi:
618 10.1002/cyto.a.22577
- 619 Lesniak A., Salvati A., Santos-Martinez M. J., Radomski M. W., Dawson K. A., Åberg
620 C., 2013. Nanoparticle adhesion to the cell membrane and its effect on nanoparticle
621 uptake efficiency. *J. Am. Chem. Soc.* 135, 1438–1444. 10.1021/ja309812z
- 622 Ma, Y., Huang, A., Cao, S., Sun, F., Wang, L., Guo, H., Ji, R., 2016. Effects of
623 nanoplastics and microplastics on toxicity, bioaccumulation, and environmental fate of
624 phenanthrene in fresh water. *Environ. Pollut.* 219, 166–173.
625 <https://doi.org/10.1016/j.envpol.2016.10.061>
- 626 Manfra, L., Rotini, A., Bergami, E., Grassi, G., Faleri, C., Corsi, I., 2017. Comparative
627 ecotoxicity of polystyrene nanoparticles in natural seawater and reconstituted seawater
628 using the rotifer *Brachionus plicatilis*. *Ecotoxicol. Environ. Saf.* 145, 557–563.
629 <https://doi.org/10.1016/j.ecoenv.2017.07.068>

- 630 Mattsson, K., Hansson, L.-A., Cedervall, T., 2015. Nano-plastics in the aquatic
631 environment. *Environ. Sci. Process. Impacts* 17, 1712–1721.
632 <https://doi.org/10.1039/C5EM00227C>
- 633 Merinska, D., Dujkova, Z., 2012. Polystyrene (nano)composites with possible anti-
634 bacterial effect. *Mathematical Methods and Techniques in Engineering and*
635 *Environmental Science* (ISBN: 978-1-61804-046-6)
- 636 Nasser, F., Lynch, I., 2016. Secreted protein eco-corona mediates uptake and impacts of
637 polystyrene nanoparticles on *Daphnia magna*. *J. Proteomics* 137, 45–51.
638 <https://doi.org/10.1016/j.jprot.2015.09.005>
- 639 Plastics Europe 2016. An analysis of European plastics production, demand and waste
640 data. Technical Report.
- 641 Paul-Pont, I., Lacroix, C., González Fernández, C., Hégaret, H., Lambert, C., Le Goïc,
642 N., Frère, L., Cassone, A.L., Sussarellu, R., Fabioux, C., Guyomarch, J., Albentosa, M.,
643 Huvet, A., Soudant, P., 2016. Exposure of marine mussels *Mytilus* spp. to polystyrene
644 microplastics: Toxicity and influence on fluoranthene bioaccumulation. *Environ. Pollut.*
645 216, 724–737. <https://doi.org/10.1016/j.envpol.2016.06.039>
- 646 Plastics Europe 2016. An analysis of European plastics production, demand and waste
647 data. Technical Report.
- 648 Rogach, A., Susha, A., Caruso, F., Sukhorukov, G., Kornowski, A., Kershaw, S.,
649 Möhwald, H., Eychmüller, A., Weller, H., 2000. Nano- and microengineering: 3-D
650 colloidal photonic crystals prepared from sub- μm -sized polystyrene latex spheres pre-
651 coated with luminescent polyelectrolyte/nanocrystal shells. *Adv. Mater.* 12, 333–337

- 652 Rossi, G., Barnoud, J., Monticelli, L., 2014. Polystyrene nanoparticles perturb lipid
653 membranes. *J. Phys. Chem. Lett.* 5, 241–246. <https://doi.org/10.1021/jz402234c>
- 654 Sendra, M., Yeste, P.M., Moreno-Garrido, I., Gatica, J.M., Blasco, J., 2017. CeO₂ NPs,
655 toxic or protective to phytoplankton? Charge of nanoparticles and cell wall as factors
656 which cause changes in cell complexity. *Sci. Total Environ.* 590–591, 304–315.
657 <https://doi.org/10.1016/j.scitotenv.2017.03.007>
- 658 Seoane, M., Esperanza, M., Cid, Á., 2017. Cytotoxic effects of the proton pump
659 inhibitor omeprazole on the non-target marine microalga *Tetraselmis suecica*. *Aquat.*
660 *Toxicol.* 191, 62–72. <https://doi.org/10.1016/j.aquatox.2017.08.001>
- 661 Steele, S., Mulcahy, M.F., 1999. Gametogenesis of the oyster *Crassostrea gigas* in
662 Southern Ireland. *J. Mar. Biol. Assoc. U. K.* 79, 673–686.
- 663 M. Suquet, M., Amourda, C., Mingant, C., Quéau, I., Lebrun, I., Brizard, R., 2007.
664 Setting of a procedure for experimental incubation of Pacific oyster (*Crassostrea gigas*)
665 embryos. *Aquaculture.* 273, 503-508.
- 666 Suquet, M., Labbe, C., Brizard, R., Donval, A., Le Coz, J.R., Quééré, C., Haffray, P.,
667 2010. Changes in motility, ATP content, morphology and fertilisation capacity during
668 the movement phase of tetraploid Pacific oyster (*Crassostrea gigas*) sperm.
669 *Theriogenology* 74, 111–117. <https://doi.org/10.1016/j.theriogenology.2010.01.021>
- 670 Suquet M, Labbé C, Puyo S. Haffray, P., 2014. Survival, growth and reproduction of
671 cryopreserved larvae from a marine invertebrate, the Pacific oyster (*Crassostrea gigas*).
672 *PLoS One* 9:e93486, 1-6.
- 673 Sussarellu, R., Suquet, M., Thomas, Y., Lambert, C., Fabioux, C., Pernet, M.E.J., Le
674 Goïc, N., Quillien, V., Mingant, C., Epelboin, Y., Corporeau, C., Guyomarch, J.,

- 675 Robbens, J., Paul-Pont, I., Soudant, P., Huvet, A., 2016. Oyster reproduction is affected
676 by exposure to polystyrene microplastics. *Proc. Natl. Acad. Sci.* 113, 2430–2435.
677 <https://doi.org/10.1073/pnas.1519019113>
- 678 Ter Halle, A., Jeanneau, L., Martignac, M., Jardé, E., Pedrono, B., Brach, L., Gigault, J.,
679 2017. Nanoplastic in the North Atlantic Subtropical Gyre. *Environ. Sci. Technol.*
680 *acs.est.7b03667*. <https://doi.org/10.1021/acs.est.7b03667>
- 681 Varela, J.A., Bexiga, M.G., Åberg, C., Simpson, J.C., Dawson, K.A., 2012. Quantifying
682 size-dependent interactions between fluorescently labeled polystyrene nanoparticles and
683 mammalian cells. *J. Nanobiotechnology* 10, 39. [https://doi.org/10.1186/1477-3155-10-](https://doi.org/10.1186/1477-3155-10-39)
684 [39](https://doi.org/10.1186/1477-3155-10-39)
- 685 Velev, O.D., Kaler, E.W., 1999. In situ assembly of colloidal particles into miniaturized
686 biosensors. *Langmuir* 15, 3693–3698. <http://dx.doi.org/10.1021/la981729c>.
- 687 Verwey, E. J. W., Overbeek, J. T. G., and Overbeek, J. T. G. 1999. Theory of the
688 stability of lyophobic colloids. Courier Corporation
- 689 Zilli Loredana; Schiavone, R.V.S., 2016. Role of protein
690 phosphorylation/dephosphorylation in fish sperm motility activation: State of the art and
691 perspectives. *Aquaculture* 472, 73–80.
692 <https://doi.org/10.1016/j.aquaculture.2016.03.043>

Figure 1. Nanoplastics characterization using Dynamic Light Scattering (A, B) and Transmission Electronic Microscopy (TEM) imaging (C, D). Size distribution of 100 nm PS-COOH (A) and 100 nm PS-NH₂ (B) measured in triplicates (each replicate is marked in blue, red and green) using a Zetasizer Nano Series software 6.2. TEM observations of 100 nm PS-COOH (C) and 100 nm PS-NH₂ (D) are also presented. Scale bar: 50 nm.

Figure 2. Confocal fluorescence microscopy carried out in fixed samples of control spermatozoa and oocytes (A, B) and spermatozoa/ oocytes exposed to 100 mg L⁻¹ PS-COOH for 3h exposure (C, D), stained with DAPI. Control cells (A, B) showed blue fluorescence coming from the DAPI dye and they has lifelike fixative' green fluorescence due to the fixation with formaldehyde. Exposed spermatozoa (C) evidenced high green fluorescence in the acrosome and in some points along the tale, coming from the aggregates of nanoplastics attached to the cell. Exposed oocytes (D) head fluorescence green coming from nanoplastics aggregates wrapped into the organic debris.

Figure 3. Intracellular reactive oxygen production (ROS) of individual' (n=6) spermatozoa after 1 h, 3 h and 5 h exposure to 4 different concentrations of PS-COOH. Significant differences between treatments are marked with lowercase letters.

SUPPLEMENTARY MATERIAL

Supplementary Figure 1 Histograms for SYBRgreen staining analysis of one female exposed to PS-COOH (1A) and PS-NH₂ (1B) for 1 h. Levels of green fluorescence is represented in X-axis in arbitrary units (A.U) and cell count (Y-axis). Each concentration is given as a type line. The fluorescence of the highest NPs concentration (100 mg L⁻¹), marked with a red area, was significantly different of the rest of treatments for both, PS-COOH and PS-NH₂ ($P < 0.001$ and $P < 0.001$; ANOVA) respectively. Control treatment are marked with a green area. Statistical analyses were performed on all females (n=6), only one females was presented as example.

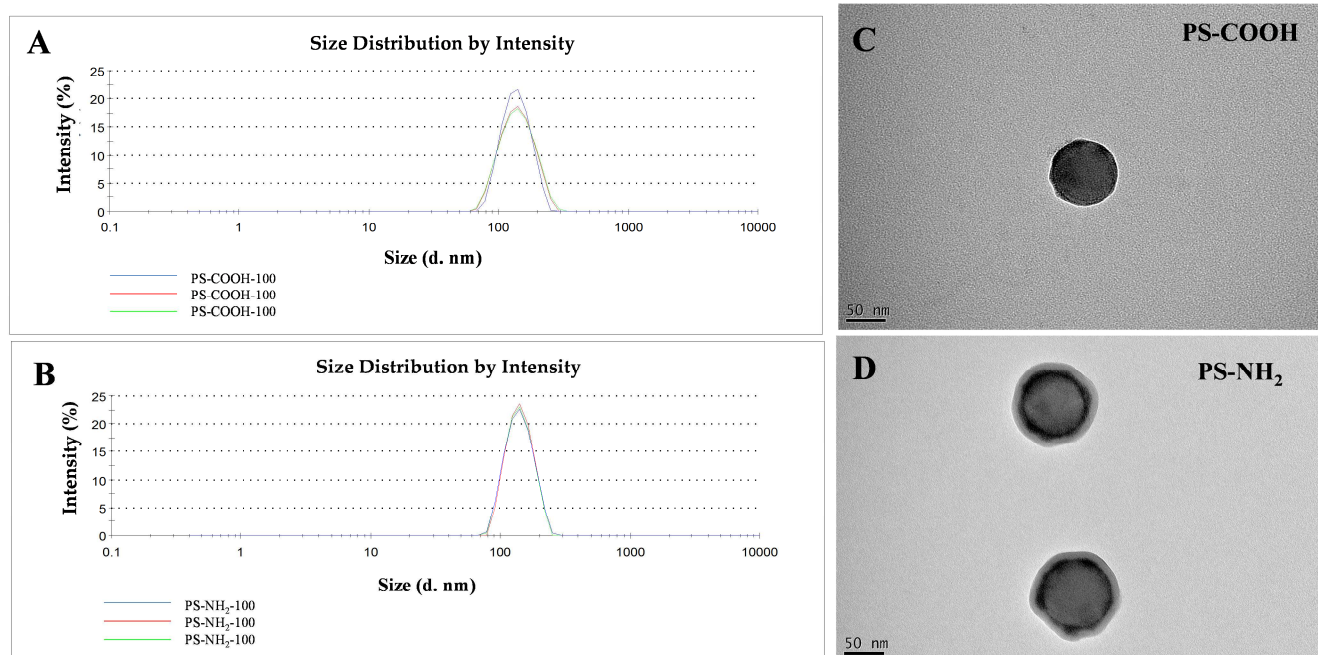
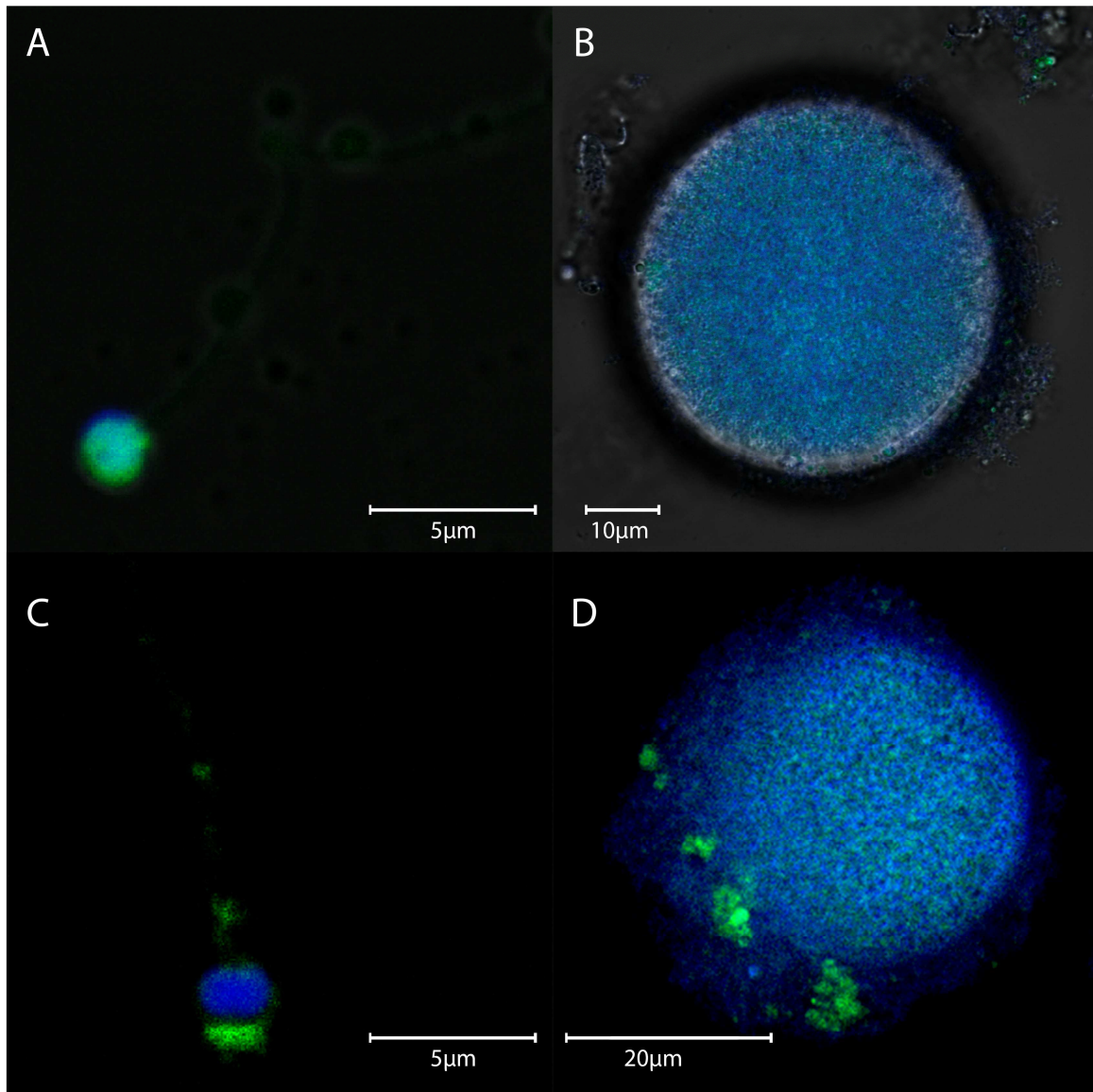


Figure 1



ACC

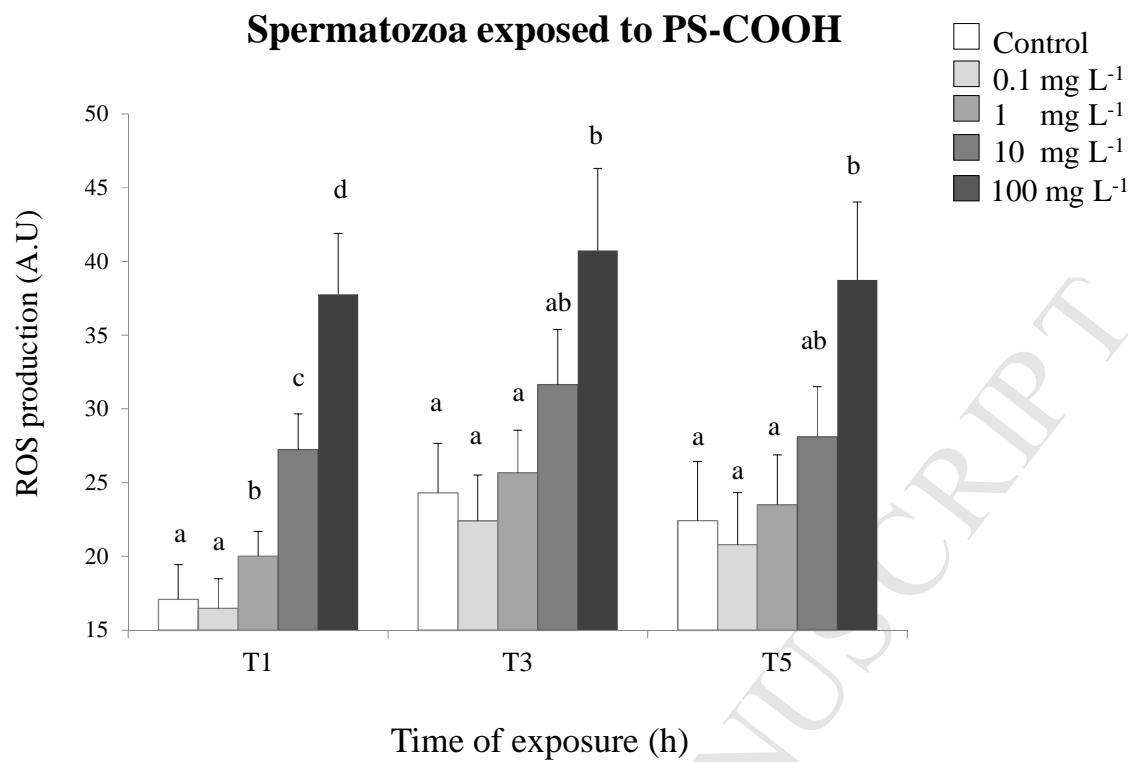


Figure 3.